J Mater Sci: Mater Med (2011) 22:1279–1291
DOI 10.1007/s10856-011-4300-0

Hyaluronan-based heparin-incorporated hydrogels for generation of axially vascularized bioartificial bone tissues: in vitro and in vivo evaluation in a PLDLLA–TCP–PCL-composite system

Subha N. Rath · Galyna Pryymachuk · Oliver A. Bleiziffer · Christopher X. F. Lam · Andreas Arkudas · Saey T. B. Ho · Justus P. Beier · Raymund E. Horch · Dietmar W. Hutmacher · Ulrich Kneser

Received: 4 November 2010 / Accepted: 16 March 2011 / Published online: 30 March 2011

Abstract Smart matrices are required in bone tissue-engineered grafts that provide an optimal environment for cells and retain osteo-inductive factors for sustained biological activity. We hypothesized that a slow-degrading heparin-incorporated hyaluronan (HA) hydrogel can preserve BMP-2; while an arterio–venous (A–V) loop can support axial vascularization to provide nutrition for a bioartificial bone graft. HA was evaluated for osteoblast growth and BMP-2 release. Porous PLDLLA–TCP–PCL scaffolds were produced by rapid prototyping technology and applied in vivo along with HA-hydrogel, loaded with either primary osteoblasts or BMP-2. A microsurgically created A–V loop was placed around the scaffold, encased in an isolation chamber in Lewis rats. HA-hydrogel supported growth of osteoblasts over 8 weeks and allowed sustained release of BMP-2 over 35 days. The A–V loop provided an angiogenic stimulus with the formation of vascularized tissue in the scaffolds. Bone-specific genes were detected by real time RT-PCR after 8 weeks. However, no significant amount of bone was observed histologically. The heterotopic isolation chamber in combination with absent biomechanical stimulation might explain the insufficient bone formation despite adequate expression of bone-related genes. Optimization of the interplay of osteogenic cells and osteo-inductive factors might eventually generate sufficient amounts of axially vascularized bone grafts for reconstructive surgery.

Abbreviations

HA	Hyaluronic acid/hyaluronan hydrogel
BMP	Bone morphogenetic protein
CT	Computerized tomography
A–V	Arterio–venous
PLDLLA	Poly(L-lactide-co-D,L-lactide)
PCL	Poly(ε-caprolactone)
TCP	β-Tri-calcium phosphate

1 Introduction

Bone tissue engineering is based on the application of mechanically stable osteo-conductive scaffolds, osteogenic cells, and osteo-inductive growth factors [1]. Although autologous bone grafts represent the gold standard for the treatment of bone defects, a number of approaches employing osteo-conductive biomaterials had been described recently, in particular when massive bone loss was present. The creation of large constructs with full viability and functional activity still presents a major challenge. Since cells cannot survive at a distance of more than

S. N. Rath · G. Pryymachuk · O. A. Bleiziffer · A. Arkudas · J. P. Beier · R. E. Horch · U. Kneser (✉)
Department of Plastic and Hand Surgery, University of Erlangen Medical Center, Krankenhausstrasse 12, 91054 Erlangen, Germany
e-mail: Ulrich.kneser@uk-erlangen.de

S. N. Rath · C. X. F. Lam
Division of Bioengineering, National University of Singapore, 21 Lower Kent Ridge Road, Singapore 119077, Singapore

S. T. B. Ho
Graduate Programme in Bioengineering, Yong Loo Lin School of Medicine, National University of Singapore, 28 Medical Drive, Singapore 117456, Singapore

D. W. Hutmacher
Faculty of Engineering, Faculty of Science, Institute of Health and Biomedical Innovation, Queensland University of Technology, Brisbane, QLD 4000, Australia

200–500 μm from a capillary, it is imperative for tissue-engineered grafts to be well perfused by a rich vascular network [2, 3]. In addition to the survival of cells, vascularization is pre-requisite even for their differentiation [4].

In the majority of cases, host blood vessels grow into a biomaterial in a random fashion after implantation in vivo, a process called extrinsic vascularization. Transfer to the defect site, though possible, is usually associated with destruction of the vascular network. Thereafter, random network formation among graft and host capillaries is essential for the survival of the graft. On the contrary, a graft pre-vascularized with a surgically created A–V loop forms an axially vascularized tissue [5]. This type of vascularization is desired by reconstructive surgeons because, similarly as in free flap transfer, it can be transferred to the defect site using microsurgical techniques [6]. After implantation, these tissues are immediately vascularized with complete survival of the graft. An axially vascularized bioartificial bone graft was successfully generated recently by our group using an A–V loop as a vascular carrier [5]. The same technology might be further extended for a large bone graft in a sheep model [7], with the addition of suitable osteo-inductive factors.

Bone induction is a complex process involving chemotaxis, mitosis, and differentiation orchestrated by a number of cytokines and growth factors in a sequential manner starting from wound healing to bone remodeling [8]. A typical bone induction process takes almost 28 days after bone loss, with the mesenchymal stem cell (MSC) attachment on day three, while vascular invasion starting on day nine [9]. The chemotactic factors induce migration of osteo-progenitor cells to the local site followed by induction of differentiation towards bone lineage and secretion of bone matrix proteins by bone-inducing growth factors, especially BMP-2. Additional BMP group of proteins and VEGF govern cell proliferation and bone vascularization to make viable osseous tissue [8].

Bone morphogenetic proteins (BMP-2 s) are part of the TGF-β group of highly active osteoinducing proteins and they played a key role in the creation of many tissue engineered bone grafts in the past [10, 11]. Considering its highly potent action, a controlled release in vivo is imperative and deviation of the release in any side can either result in insufficient bone formation or lead to undesired ectopic bone formation, compromising the vitality of nearby tissues [11, 12]. Within 14 days of local BMP-2 application, its concentration decreases to 5% of initial dosage [13]. When BMP-2 is applied as a solution in vivo, it is released into the blood stream and loses its bioactivity within hours after rapid degradation and may not be effective for bone induction [14].

One major goal for drug delivery systems is to maintain BMP-2 at the site of bone loss and release it in a controlled and continuous manner to act on migrating osteogenic cells to induce bone formation [13]. The release has to be predictable and at physiological concentrations; the BMP-responsive cells should be located nearby. Failure of clinical trials has been reported when its bioavailability was lower than the physiological requirement of the bone healing process because of its rapid degradation after release [15]. To circumvent the problem, increased amounts of BMP-2 at supra-physiologic doses may be given. In addition to increased cost, this may induce ossification impinging on nearby vital neurovascular structures and life-threatening swelling and disability [16]. Though type I collagen is most commonly used for BMP-2 as a carrier [11], a number of other carrier systems have been suggested [13]. In some cases, carrier systems such as fibrin glue are used to inhibit BMP-2 diffusion out of the applied site to prevent soft tissue ossification [12]. Additionally, a carrier acts more than just delivering BMP-2 with documented supra-additive effect of a carrier and BMP-2 forming a favorable three-dimensional extracellular matrix.

Hyaluronan (HA) hydrogel is osteo-conductive and osteo-integrative. However, for its osteo-inductive action, special growth factors need to be applied. Currently, BMP-2 and BMP-7 have been approved with type I collagen carrier, but other carriers may be superior in terms of efficacy [17]. Hyaluronan has been shown to protect growth factors in vitro for more than 4 weeks from proteolysis [18]. It has also been shown to release active growth factors slowly in the presence of heparin [18]. Heparin can prolong the stability of BMP-2 almost 20-fold and can produce ectopic bone with only 1 μg of BMP-2, avoiding the use of significantly increased doses [19]. However, for the effective action of BMP-2, angiogenesis and vascular invasion must precede before ossification [9]. Exploiting the ability of BMP-2 to induce ectopic bone, heparin-incorporated hyaluronic acid hydrogel can be utilized for its delivery.

In this experiment, we hypothesize that an axially vascularized ectopic tissue-engineered bone graft can be fabricated with an A–V loop surrounding the PLDLLA–TCP–PCL-Hyaluronan scaffold-hydrogel composite. The aim of this study was twofold: firstly, to evaluate the BMP-2 release capacity of the system and growth and survival of primary osteoblasts in vitro; secondly, to investigate progress of vascularization and formation of bone tissue within the composites in vivo following application of different concentrations of BMP-2 or primary osteoblasts.

2 Materials and methods

2.1 Scaffold fabrication

The scaffolds were fabricated using the fused deposition modeling (FDM) principle [20] utilizing three different

materials: PLDLLA (Boehringer-Ingelheim, Ingelheim am Rein, Germany), PCL (Absorbable Polymers, US), TCP (Progentix, MB Bilthoven, Netherlands), in a ratio of 64, 16, and 20% by weight, respectively. The strength is provided by the bioceramic component, while the polymer part enables plasticity and ease of fabrication. The fabrication was by an in-house rapid prototyping (RP) system, namely the screw extrusion system (SES), similar to FDM [20]. The details of the fabrication method are described elsewhere [21]. Briefly, it exploits a layer-by-layer fabrication technique to assemble three-dimensional (3D) structures by depositing two-dimensional (2D) supporting struts based on specified lay-down patterns to assemble the whole structure. Material is fed into the top of the barrel chamber, heated to a molten liquefied state at 120°C and transported towards a 400 μm nozzle with aided displacement and pressure from the turning screw feed.

Scaffold sheets of 50 × 50 × 1.5 mm^3 were fabricated with a 0–90° lay-down pattern. Discs with 8 mm diameter were punched out from it and fabricated into bobbin-shaped constructs (Fig. 1). The scaffolds were uniformly treated with 5 M sodium hydroxide for 5 min and rinsed with de-ionized water to yield a hydrophilic and corrugated surface for improved cell attachment [22]. They were sterilized in 70% ethanol overnight followed by UV light for 2 h. The biomechanical properties of a comparable composite scaffold were found to be suitable for bone tissue engineering, showing excellent compatibility with MSCs [21].

2.2 Osteoblast culture and analysis in hyaluronan-based hydrogel

Primary osteoblasts were isolated from long bones of male Lewis rats as described elsewhere [23]. In brief, after sacrificing the rats at 4–8 weeks age, the long bones were collected and serially digested in sterile collagenase-II (554 U/ml, Biochrom AG, Berlin, Germany) in 1× PBS. Subsequently, the cells were cultured in flasks (COSTAR, Cambridge, USA), maintained at 37°C and 5% CO_2 with twice weekly media change. Only second passage cells were seeded into the scaffold for in vitro and in vivo evaluation.

The hyaluronan-based (HA) hydrogel (Extracel-HP, Glycosan BioSystems, Salt Lake City, Utah) was supplied as a kit consisting of three components, namely thiol-modified hyaluronan and heparin, thiol-modified gelatine, and thiol-modified cross-linker, polyethylene glycol diacrylate. The components were prepared with distilled water at 37°C under aseptic conditions and were mixed at 2:2:1 ratio, respectively, according to the manufacturer's recommendations. The osteoblasts were mixed in the hydrogel such that 100 μl of the hydrogel, aliquoted in each well of 96-well culture plate, contained 10,000 osteoblasts. The cells were cultured in a 37°C incubator with 5% CO_2 with 100 μl of media. The medium was changed twice weekly. Osteoblasts in HA were observed for 8 weeks under inverted light microscope (Leica DMIL, Weltzlar, Germany).

The hyaluronan-osteoblast specimens were analyzed by AlamarBlue (Biosource Int., Camarillo, CA) assay. Each week, culture medium was aspirated and 150 μl of culture medium with 5% AlamarBlue was added to the specimens and incubated for 4 h at 37°C. Absorbance was then measured with a plate reader (SPECTRAmax 190, Molecular Devices, Sunnyvale, CA, USA) at wavelengths of 570 and 600 nm. The percentage of AlamarBlue reduction was subsequently calculated as advised by the manufacturer.

Cell proliferation was evaluated using PicoGreen DNA quantification assay (Molecular Probes, Invitrogen GmbH, Karlsruhe, Germany) at 4 and 8 weeks as advised by the manufacturer. Specimens were thoroughly destroyed with lysis buffer (10 mM Tris (pH 7.0), 1 mM EDTA, and 0.2% v/v triton X-100; all from Sigma-Aldrich GmbH, Steinheim, Germany). Fluorescence of specimen wells was measured with a fluorescent microplate reader (Genios, Tecan Group Ltd, Maennedorf, Switzerland) at excitation and emission wavelengths of 485 and 535 nm, respectively, corrected with blanks.

To visualize viable and non-viable cells, osteoblasts were labeled with fluorescent probes. The osteoblast-seeded hydrogels were washed with 1× PBS and incubated with 2 μg/ml fluorescein diacetate (FDA) (Molecular Probes Inc., Eugene, USA) in 1× PBS, for 15 min at 37°C.

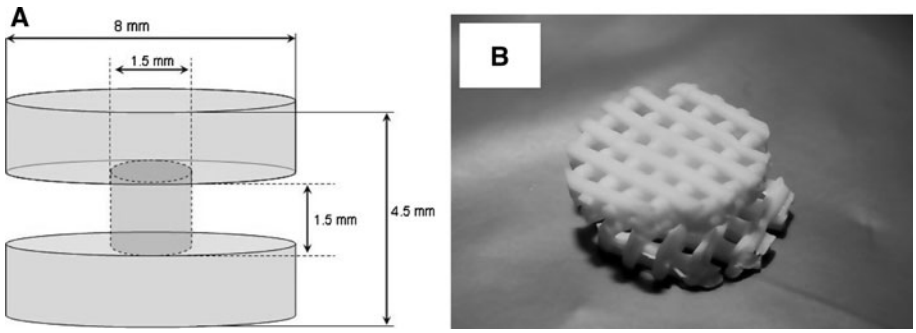

Fig. 1 **a** Schematic diagram of the bobbin-shaped scaffold. **b** The scaffold showing high porosity and a central groove for accommodating the A–V loop

They were gently rinsed twice in 1× PBS and placed in 20 μg/ml propidium iodide (PI) solution (Invitrogen GmbH, Karlsruhe, Germany) for 2 min at room temperature. After thorough rinsing in 1× PBS, the specimens were kept in 1× PBS and viewed under a fluorescent microscope (Axiovert 25, Carl-Zeiss AG, Goettingen, Germany). The viable cell cytoplasms were labeled green, while non-viable cell nuclei were labeled red.

2.3 Release kinetics of rhBMP-2 from hyaluronan-based hydrogel

The rhBMP-2 (INFUSE bone graft, Medtronics, Minneapolis, USA) was reconstituted to final concentration of 3.33 μg/μl in PBS. 10 μg of rhBMP-2 was incorporated in 50 μl of hyaluronan hydrogel. All disc shaped hydrogels were uniformly polymerized to get a thickness of 4 mm and a diameter of 5 mm. The BMP-2 containing hydrogel discs ($n = 3$) were placed in 1 ml of pre-warmed PBS until 35 days from the start of the experiment. At different time points (1, 2, 4, 6, and 24 h and 2, 4, 7, 10, 14, 17, 21, 28, and 35 days), 100 μl of PBS were sampled and replaced with an equal amount of fresh PBS after the scaffolds were kept on a shaker for 3 min. The collected 100 μl of PBS were kept in −80°C and the rhBMP-2 content was measured by rhBMP-2 ELISA kit (Quantikine, R&D systems, Minneapolis, MN, USA). The values were calculated from the standard curve. The cumulative release was calculated for each time point.

2.4 In vivo experiments

Twenty-four inbred male Lewis rats (Charles-River, Sulzfeld, Germany) weighing 200–300 g were used with approval by the animal care committee of the University of Erlangen and the Government of Mittelfranken, Germany. Animals were kept in 12 h dark–light cycle with free access to standard chow (Altromin, Hamburg, Germany) and water at the veterinary care facility of the University of Erlangen Medical Center. All operations were performed by experienced microsurgeons using a surgical microscope (Karl Zeiss, Jena, Germany) under general anaesthesia with Isoflurane (Baxter, Unterschleißheim, Germany).

The rats were divided into four groups, each consisting of six animals. The PLDLLA–TCP–PCL scaffold was loaded with 1 ml of HA hydrogel containing either of 500 ng rhBMP-2 (group A), 2.5 μg rhBMP-2 (group B), or three million hydrogel-immobilized osteoblasts (group C) prior to implantation. Scaffolds with plain HA hydrogel served as controls (group D).

The surgical technique has been described previously by our group [24]. In brief, the femoral vessels and nerve were exposed by a longitudinal incision from the inguinal ligament to the knee. The sheath of the neurovascular bundle was opened. After exposure of the right-sided femoral vessels, a 20 mm vein graft was harvested from the right femoral vein. An A–V loop was created by interposition of the vein graft between the left sided femoral artery and the left femoral vein with interrupted non-absorbable 11-0 nylon stitches (Ethilon, Ethicon GmbH, Norderstedt, Germany). The A–V loop was placed around the PLDLLA–TCP–PCL scaffold and the whole construct was placed into a sterile cylindrical Teflon-chamber (inner diameter 10 mm, height 6 mm, constructed by the Institute of Materials Research, Division of Glass and Ceramics, University of Erlangen). The chamber was then capped and fixed to the underlying muscle. The skin was closed using interrupted 3-0 vicryl sutures (Ethicon GmbH, Norderstedt, Germany). All animals received 0.2 ml benzylpenicillinbenzathine (Tardomycel; Bayer, Leverkusen, Germany), buprenorphine (0.3 mg/kg rat weight) (Temgesic; Essex Chemie AG, Luzern, Switzerland), and heparin (80 IU/kg) (Liquemin; Ratiopharm, Ulm, Germany) postoperatively.

Explantation of the specimens was performed after 8 weeks. For sacrifice, one specimen from each group was used for RNA isolation as described later. The other rats were perfused with Microfil under general anesthesia for micro-CT analysis. The aorta was cannulated and the vascular system was rinsed with heparinized Ringer solution (100 IU/ml) under hydrostatic pressure. The distal vascular system was then injected with 20 ml microfil (MV-122) containing 5% of MV curing agent (both from Flowtech, MA, USA) as advised by the manufacturer. Finally the aorta and caval vein were ligated and the rats were cooled at 4°C for 24 h. Specimens were explanted in toto and fixed in 3.5% formalin solution before micro-CT.

2.5 Micro-CT analysis

For each of the experimental groups, two specimens were selected at random for micro-CT analysis. To decalcify the scaffolds, the explanted grafts were treated with 20% EDTA for 3 weeks before further manipulation. They were subsequently scanned on a high resolution ''ForBild'' scanner (an in vivo micro computerized tomography (micro-CT) scanner developed by Institute of Medical Physics, FAU Erlangen-Nuremberg, Germany). The constructs were scanned with following parameters: Al-0.5 mm filter, tube voltage of 40 kV, 15 μm pixel size, and 15 μm slice distance between consecutive slices. The data were volumetrically re-constructed using ImpactView software (Vamp GmbH, Erlangen, Germany) in a 1024 × 1024 pixels matrix. Further, 3D modeling for data analysis was done using Mimics v8.02 software (Materialise, Leuven, Belgium). The different tissues were segmented according

to their Hounsfield Unit values by global thresholding procedure to selectively obliterate the scaffolds and soft tissues. After 3D reconstruction, the volume and area of microfil-perfused blood vessels were calculated. Using the data, the mean number of vessels per unit length was calculated, as described before [25].

2.6 Histology and histomorphometry

The samples were serially dehydrated and paraffin embedded according to standard protocols. Five μm sections were taken using a microtome (Leica RM 2135, Wetzlar, Germany). All the slides were stained with Hematoxylin and eosin (H & E) using a fully automated process (Jung Auto Stainer XL, Leica Microsystems, Nussloch, Germany).

Immunhistochemical analysis was performed using rabbit polyclonal antibodies against vWF (von-willebrand factor) (A0082, Dakocytomation, Carpinteria, CA, USA) at 1:500 dilution to confirm the vascular endothelium. Envision HRP anti-rabbit kit (K4011, Dakocytomation, Carpinteria, CA, USA) was used as secondary antibody.

The histomorphometric analysis was performed by two blinded, independent observers as described elsewhere [26]. Briefly, the images of two standardized planes (500 μm proximal and 500 μm distal to the central plane) were photographed and oriented perpendicular to the longitudinal axis of A–V loops. All images were taken by a light microscope with bright-field filter (Leica DM IRB, Wetzlar, Germany) and digital camera under ×25 magnification. The individual images of each cross section were set together (Photoshop, Adobe, San Jose, CA, USA). The composed images were rendered bimodal (ImageJ, NIH, Bethesda, MA, USA). The construct size (cross-sectional area) and the area of FVT were measured for each of the sections. The percentage of fibro vascular tissue (% FVT) was calculated by the ratio of total FVT area to total cross sectional area of the specimen. The total number of blood vessels was assessed by counting the microfil-filled (positive) vessels in ten pre-selected fields of view (four in the central region and three each in upper and lower parts of the construct) at ×100 magnification. Results are expressed as means ± standard-errors of the mean.

2.7 RNA isolation and quantitative real time RT-PCR

After scarification of the animal, the chamber was quickly isolated and kept overnight at 4°C in RNAlater RNA Stabilization Reagent (Qiagen, Hilden, Germany) and further in −80°C until RNA isolation. Total RNA was isolated from the tissue grown in the loop using TRIzol Reagent (Invitrogen, Carlsbad, CA, USA) followed by RNeasy Mini Kit (Qiagen, Hilden, Germany) according to manufacturer's protocol and RNA was measured by BioPhotometer (Eppendorf, Hamburg, Germany). Total RNA was converted to c-DNA using oligo d-T primers (Fermentas, Glen Burnie, MD, USA) and RevertAid H Minus M-MuLV Reverse Transcriptase (Fermentas, Glen Burnie, MD, USA).

The amount of cDNA corresponding to 20 ng of total RNA was then analyzed in triplicates by semi-quantitative real time PCR for selected genes with primers as shown in Table 1 by Mx3000P QPCR System (Stratagene, Agilent technologies, La Jolla, CA, USA). The gene expressions were normalized to internal β-actin expression and the relative fold change was expressed by comparing to that of control group D.

2.8 Statistical analysis

Statistical comparisons were performed for histomorphometric analysis by a two-way ANOVA test followed by Bonferroni's post-test (Sigmastat v3.5, Chicago, IL) considering significant difference at the 95% confidence interval. Standard error bars were included in all graphs and represent the 95% confidence interval. For all pairwise comparisons on quantitative results the Student's *t*-test was used with a confidence level of 95% ($P < 0.05$).

3 Results

3.1 Osteoblasts in hyaluronan-based hydrogel in vitro

At 4 and 8 weeks, osteoblasts were relatively distinct and well maintained throughout the hydrogel (Fig. 2a). However, the thickness of the hydrogel decreased considerably over 8 weeks. Vitality of osteoblasts was demonstrated over the entire observation period by FDA/PI staining (Fig. 2b) while dead cells were almost non-existent.

The metabolic activity of the cells increased progressively until week five followed by a decline by week eight (Fig. 2c). A similar trend was observed in the DNA quantification assay, where a significant decrease in dsDNA values between week four (35.38 ± 10.34) and week eight (7.57 ± 1.90) was demonstrated (Fig. 2d).

3.2 Release kinetics of BMP-2 from hyaluronan-based hydrogel

In vitro BMP-2 release from HA hydrogels was followed until day 35 (Fig. 3). The release kinetics of BMP-2 was characterized by a fast initial peak within the first 3 days followed by a sustained release over the course of 35 days. Even at the end of 5 weeks, a considerable percentage of BMP-2 was still incorporated inside hydrogel. Within the first 24 h, almost 10% of the loaded BMP-2 was released.

Table 1 The primers of the genes analyzed by real time PCR

Gene name	Forward primer	Reverse primer
Alkaline phosphatase	GCTGATCACTCCCACGTTTT	GCTGTGAAGGGCTTCTTGTC
Biglycan	CCACCAACTAACCAGCCTGT	CAAGGTGAAGTCCCAGAAGC
Syndecan	CTGATCCTGCTGCTGGTGTA	TCATGCGTAGAACTCGTTGG
BMP 2	TGAACACAGCTGGTCTCAGG	TTAAGACGCTTCCGCTGTTT
Osteocalcin	CTATGGCACCACCGTTTAGG	AGCTGTGCCGTCCATACTTT
Collagen 1	TTCTGAAACCCTCCCCTCTT	CCACCCCAGGGATAAAAACT
Osteonectin	AAACATGGCAAGGTGTGTGA	AAGTGGCAGGAAGAGTCGAA
Agrrecan	AACTCAGTGGCCAAACATCC	AGATGTTCCCTCACCAGTGC
Collagen 2	CGAGGTGACAAAGGAGAAGC	AGGGCCAGAAGTACCCTGAT
VEGF	AATGATGAAGCCCTGGAGTG	ATGCTGCAGGAAGCTCATCT
Beta-actin	GATCATTGCTCCTCCTGAGC	ACATCTGCTGGAAGGTGGAC
FGF 2	TTCTTTGAACGCCTGGAGTC	CCGTTTTGGATCCGAGTTTA

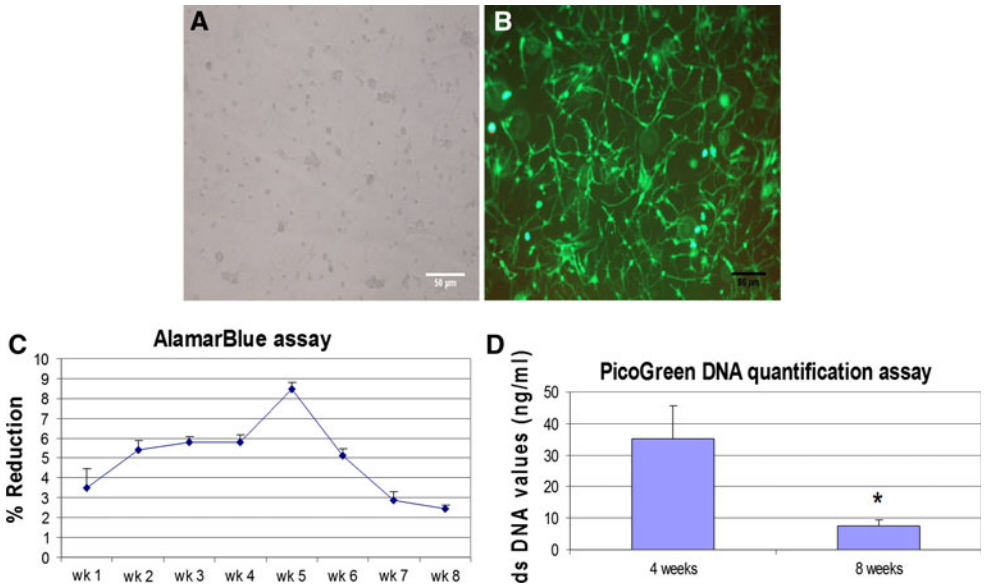

Fig. 2 Osteoblasts in hyaluronic acid hydrogel after 4 weeks, examined in **a** inverted light microscope, and **b** after FDA/PI staining in fluorescence microscope. Cells are evenly distributed within the matrix and display a typical and differentiated morphology. There are virtually no dead (PI-positive) cells. **c** Metabolic activity of osteoblasts is demonstrated by AlamarBlue assay in hyaluronic acid hydrogel over the observation period with a peak at week five. **d** The dsDNA value of osteoblasts is significantly decreased at week eight compared to week four as evidenced by PicoGreen assay ($P < 0.05$)

Thereafter, the release rate was almost constant until the end of observation.

3.3 Qualitative and quantitative micro-CT analysis

The pattern and distribution of angiogenesis of representative samples in micro-CT scanning are shown for scaffolds with plain hydrogel (control group D, Fig. 4d), hydrogel with low dose BMP-2 (500 ng, group A, Fig. 4a), hydrogel with high dose BMP-2 (2.5 μg, group B, Fig. 4b), and hydrogels containing osteoblasts (group C, Fig. 4c). In

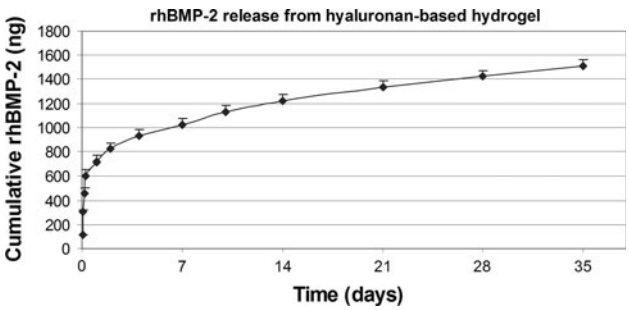

Fig. 3 Cumulative release of rhBMP-2 from the hyaluronic acid hydrogel over a period of 35 days

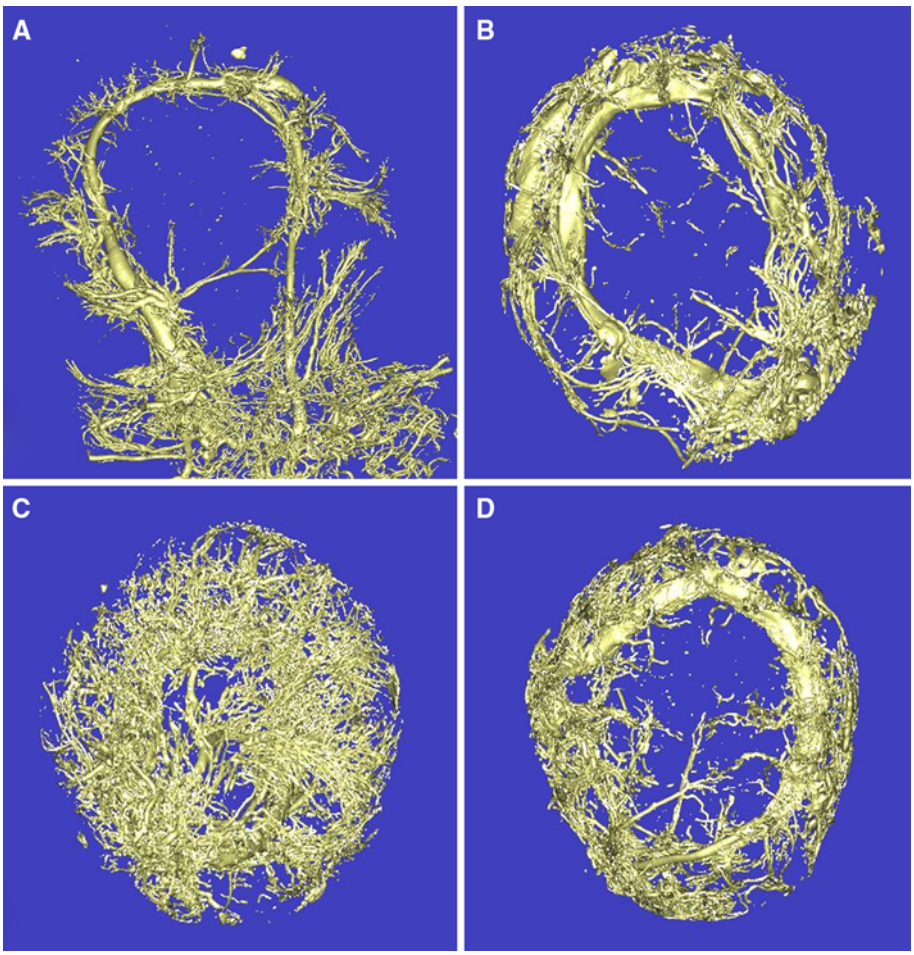

Fig. 4 Micro-CT analysis. 3D reconstructed images of representative samples from **a** group A (500 ng/ml BMP-2), **b** group B (2.5 μg/ml BMP-2), **c** group C (osteoblast transplanted), and **d** group D (control). Osteoblast transplantation leads to considerable increase in blood vessel outgrowth from the A–V loop

groups A and D, blood vessels start sprouting from the A–V loop into the centre of the scaffold. In group B, the newly grown vessels already extend towards the centre of the scaffold from all directions. However, only in group C (osteoblast transplantation) there is extensive vascular growth filling the entire centre of the scaffold (Fig. 4d).

The total volume of angiogenesis approached 5–10 mm^3 in control group D as well as groups A and B (low dose BMP-2 and high dose BMP-2, respectively) (Fig. 5a). However, in group C (osteoblast transplantation) the value was 10–15 mm^3. As per the calculation by Bolland et al. [25], the number of vessels per mm length in groups A, B, and D is within 10–100, while one group C sample shows 187 per mm length (Fig. 5b). No further statistical analysis of the micro-CT data was performed due to the limited number of samples (Fig. 5b).

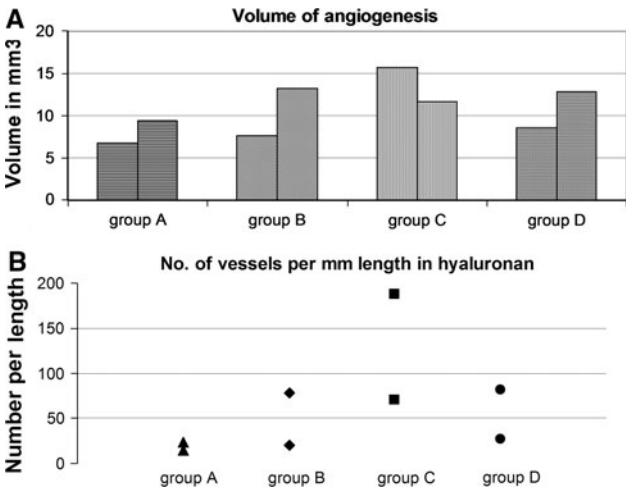

Fig. 5 Quantitative micro-CT analysis of specimens after 8 weeks in vivo ($n = 2$ per group) showing **a** the volume of angiogenesis in the isolation chamber, and **b** number of vessels per mm length

3.4 Histology and immunohistochemistry

Histological specimens showed numerous microfil-filled blood vessels (black) in specimens from all groups. A dense network of newly formed blood vessels originated from the A–V loop and progressively invaded the void spaces within the scaffolds from all groups. However, BMP-2 concentration and transplantation of osteoblasts influenced the number of blood vessels and the volume of newly formed fibro-vascular tissue. A representative figure

of each type of sample is shown in Fig. 6: low concentration of BMP-2 (group A, Fig. 6a), high concentration of BMP-2 (group B, Fig. 6b), osteoblast transplantation (group C, Fig. 6c), and scaffolds with plain hydrogel (control group D, Fig. 6d). There was no significant foreign body reaction detectable in specimens from any group and the scaffolds were almost completely intact after 8 weeks. In specimens from groups A, B, and D (low concentration BMP, high concentration BMP and control, respectively), there was some amount of non-resorbed hyaluronan matrix observed after 8 weeks. In contrast, in specimens from group C (osteoblast transplantation), the hydrogel component was completely resorbed.

Immunostaining with vWF antibody specifically demonstrated patency and functional integrity of blood vessels with microfil-filled (black) lumen in specimens from all groups (Fig. 6e, f). There was no significant bone formation detectable in histological samples from any group.

3.5 Histomorphometry

The percentages of fibro vascular tissue (FVT) were for group A 12.57 ± 1.3, for group B 16.52 ± 0.7, for group C 24.14 ± 1.4, and for group D 16.28 ± 2.6, respectively. Similarly, the percentages of unresorbed hyaluronic acid matrix left at the end of 8 weeks were 15.34 ± 3.1, 5.76 ± 1.0, 0 ± 0, and 13.62 ± 2.1 for groups A, B, C, and D, respectively. Interestingly, the entire hyaluronic acid hydrogel was resolved in group C (osteoblast transplantation) specimens. The percentage of FVT was

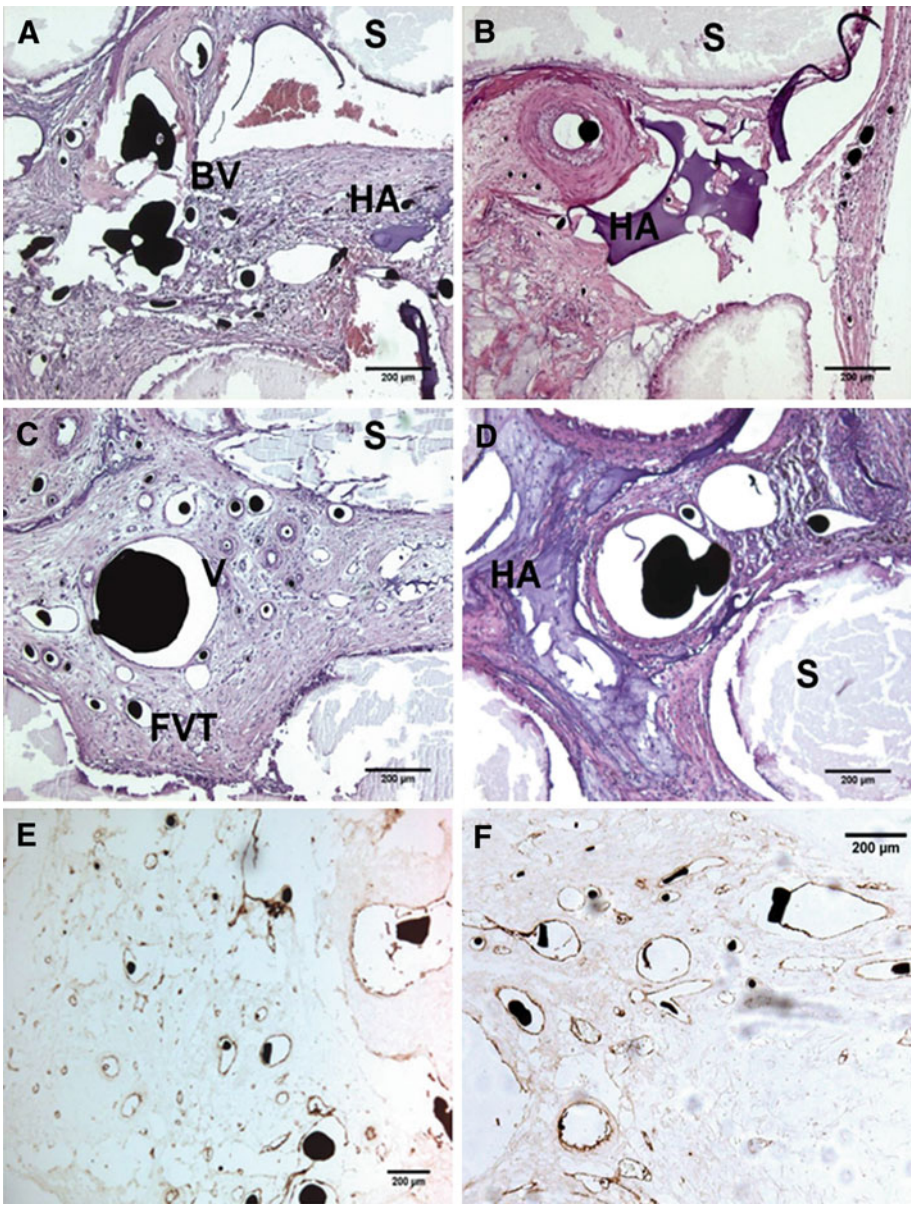

Fig. 6 Hematoxylin and eosin staining of representative specimens: **a** group A (500 ng/ml BMP-2), **b** group B (2.5 µg/ml BMP-2), **c** group C (osteoblast), and **d** control group D after 8 weeks. *S* scaffold, *HA* hyaluronic acid matrix, *BV* microfil-filled blood vessels, *FVT* fibro vascular tissue, *V* vein of the loop. All *scale bars* show 200 µm. (**e** and **f**) Immunohistochemistry with vWF antibody showing the vascular architecture of group B and group D, respectively. The co-localization of vWF-positive walls and microfil-filled lumen clearly demonstrate functional integrity of the newly grown vasculature

significantly higher ($P < 0.001$) in samples from group C in comparison to groups A, B, and D. The percentage of hyaluronic acid hydrogel matrix values was significantly lower in groups B and C compared to groups A and D. The results are displayed graphically in Fig. 7a.

The total number of blood vessels per cross section area was 95.57 ± 23.40, 66.40 ± 3.91, 138.7 ± 9.60, and 67.33 ± 12.03 in groups A, B, C, and D, respectively. Specimens from the osteoblast transplantation group C contained significantly more blood vessels than specimens from groups B and D ($P = <0.05$) (Fig. 7b).

3.6 Quantitative real time RT-PCR

Bone-related gene expression profile is shown in Fig. 8. Expression of collagen-I and osteonectin was not significantly increased in the experimental groups A–C in comparison to control group D. In contrast, alkaline phosphatase, RUNX-2, osteocalcin, and IBSP expressions were increased in groups A, B, and C (low-and high concentration BMP and osteoblast transplantation). However, this effect was not statistically significant for all groups.

Expression profile for selected extracellular matrix proteins and growth factors are shown in Fig. 9. Syndecan expression was neither influenced by BMP-2 nor transplantation of osteoblasts. Interestingly, biglycan expression was increased in high-concentration BMP-2 and osteoblast transplantation groups (groups B and C, $P < 0.05$ only for group B). The expression profile of growth factors such as VEGF, FGF2, and BMP-2 was not significantly different in the experimental groups A–C compared to control group D.

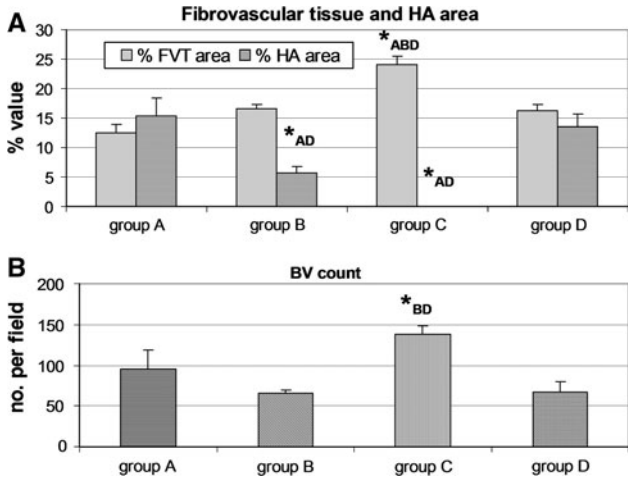

Fig. 7 Histomorphometric calculations of blood vessel formation in the graft constructs. **a** Mean percentage of FVT and non-resorbed hyaluronic acid matrix. **b** Mean number of blood vessels per cross section. *Asterisks* indicate statistically significant differences between groups ($P < 0.05$); *group A* 500 ng/ml BMP-2, *group B* 2.5 μg/ml BMP-2, *group C* osteoblast transplantation, and *group D* control

4 Discussion

This study clearly demonstrates that the hyaluronan-based matrix supported growth and differentiation of osteoblasts in vitro and in vivo and allowed sustained release of BMP-2. The whole system showed positive evidence of bone-related gene expression, though it eventually failed to induce significant amounts of bone histologically in an isolation chamber model of axial vascularization. Summarizing, PLDLLA–TCP–PCL polymer-ceramic composite scaffolds combined with HA-based hydrogel might be utilized in engineering of bio-artificial bone tissues.

Typical hydrogel systems are characterized by an initial higher peak of growth factor release followed by a reduced release later. At the beginning, there is maximal availability of free growth factors for nearby cells [27, 28]. Afterwards, two distinctive release patterns are seen for different hydrogels. In surface-eroding hydrogel, there follows a slow release later in time; while in bulk-eroding hydrogel, degradation and random release ensue [29]. Though the hydrogel is required to bind BMP-2, the continuous release must induce sufficient concentration in the vicinity to act on precursor cells to induce the specific action of the growth factor. In our study, a similar trend regarding the amount and rate of release of BMP-2 is seen at the beginning, followed by a very slow release rate until 5 weeks. The final disintegration might have released all BMP-2 contained in the hydrogel.

The hyaluronan hydrogel demonstrated in vitro growth compatibility with the osteoblasts and supported their replication, as observed in light microscopic pictures and corroborated by AlamarBlue results until week five. Thereafter, the progressive decline in AlamarBlue assay might be due to gradual dissolution of hydrogel by hyaluronidase secreted by osteoblasts with corresponding loss of cells [30]. This was substantiated by PicoGreen assay, where 8 week dsDNA was significantly lower than 4 weeks. Cell death cannot account for the lowered values as all cells were found healthy and alive in FDA/PI staining.

Successful vascularization of composite scaffolds was clearly demonstrated by micro-CT and histological analysis. In micro-CT angiograms, there was significant angiogenetic activity originating from the original A–V loop. In BMP groups (groups A and B), the proximal part of loops generally displayed comparatively more sprouting blood vessels than the distal part found interior in the chamber. This might be due to VEGF mediated vascularization by BMP-2 [31]. In osteoblast transplanted group C, there were a uniform extensive angiogenetic activity and formation of blood vessels throughout the chamber, even extending to the centers. The data were corroborated well by histomorphometric analysis. The FVT area as well as the number of blood vessels was significantly increased in

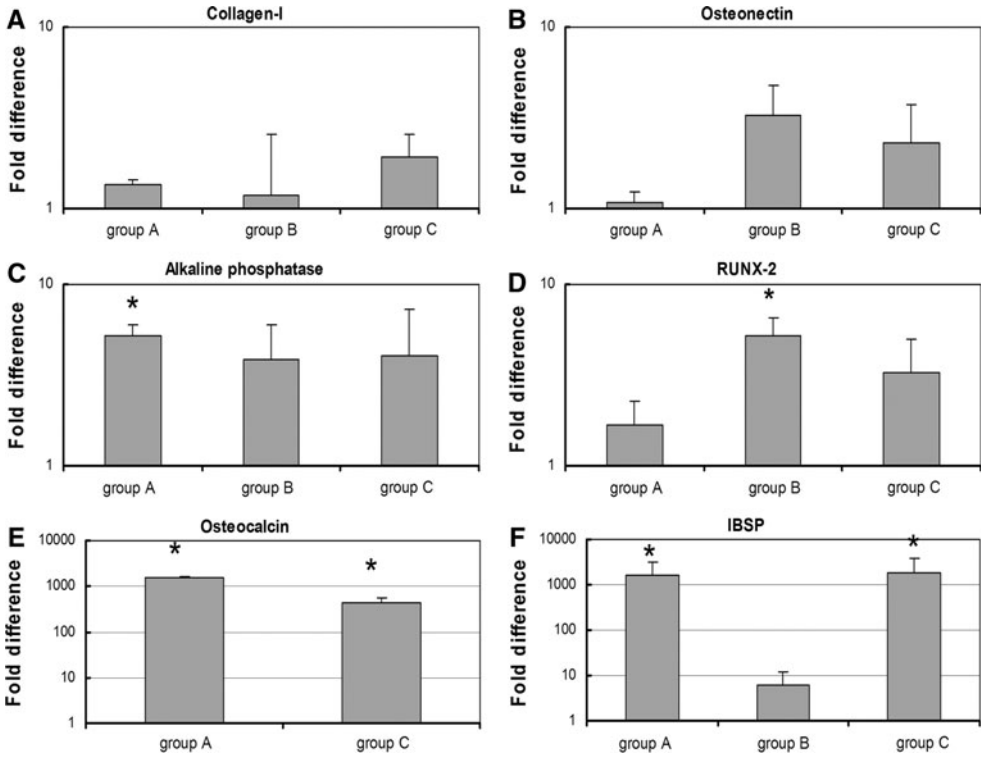

Fig. 8 Quantitative real time RT-PCR analysis of bone-related gene expression: Collagen-I (**a**), alkaline phosphatase (**b**), IBSP (**c**), RUNX-2 (**d**), osteocalcin (**e**), and osteonectin (**f**). Specific gene expression was normalized to internal β-actin expression. *Values* represent the fold change compared to control group D. The *error bar* represents standard deviation and the *asterisks* indicate significant differences between experimental groups and control group D ($P = 0.05$). Each *bar* represents three independent measurements. *Group A* 500 ng/ml BMP-2, *group B* 2.5 μg/ml BMP-2, *group C* osteoblast transplantation, and *group D* control

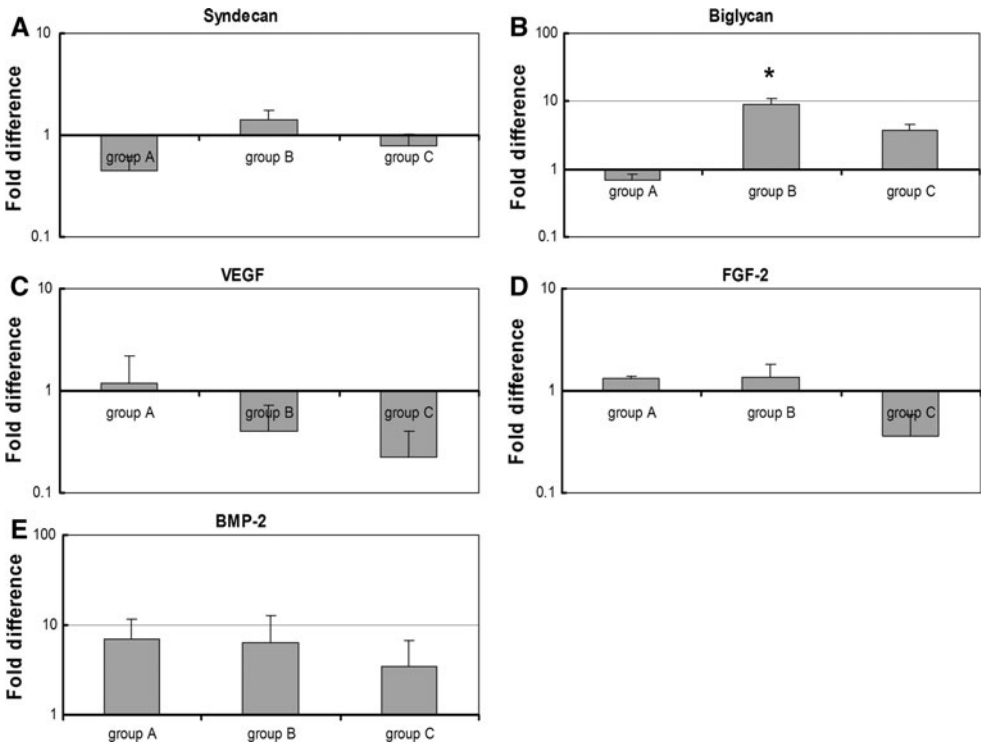

Fig. 9 Quantitative real time RT-PCR analysis of extracellular matrix and growth factors expressions: Syndecan (**a**), Biglycan (**b**), VEGF (**c**), FGF-2 (**d**), and BMP-2 (**e**). Specific gene expression was normalized to internal β-actin expression. *Values* represent the fold change compared to control group D. The *error bar* represents standard deviation and the *asterisks* indicate significant differences between experimental groups and control group D ($P = 0.05$). Each *bar* represents three independent measurements. *Group A* 500 ng/ml BMP-2, *group B* 2.5 μg/ml BMP-2, *group C* osteoblast transplantation, and *group D* control

group C specimens. These findings might be explained by faster resorption of hyaluronic acid following application of osteoblasts [30]. This is supported by significantly lower percentage of remaining hyaluronan matrix in group C specimens (Fig. 7). The degradation byproducts may stimulate angiogenesis subsequently [32]. Additionally, a strong hypoxic stimulus from cells may stimulate VEGF secretion [33].

Contrary to the demonstration of extensive vascularization, a clear histological evidence of bone formation could not be seen in the examined sections of our loop model. Researchers have tried BMP-2 dosage from 1 μg in

hind-limb muscle and subcutaneous tissue to 50 μg in bone defect sites in rats with successful bone induction [34, 35]. We have also demonstrated extensive bone formation histologically after subcutaneous application of 2.5 μg of BMP-2 after 8 weeks (data not shown). The absence of bone histology in experimental specimens might be due to ineffective dosage of BMP-2, which could only be addressed empirically. The currently approved effective dose with a collagen carrier requires BMP-2 in milligram amounts, while in vivo the level is actually in nano to pico molar range [17]. The higher BMP-2 dose might be necessary for ectopic osteoinduction, where there is no readily available effector tissue present.

Another reason might be the challenging properties of the isolation chamber model. Since the newly grown tissue was isolated from surrounding tissues except for the communication through vascular loops, the model had limited access to subcutaneous tissue. Previous studies in our model demonstrated that the neo-angiogenesis and the subsequent FVT invasion occur only after 2–4 weeks of surgical loop placement [24]. Beforehand, there might be no effector cells in the adjacent area. By this time, a large percentage of BMP-2 must have been released and biodegraded without any action. With its slow release phase after 2 weeks, the local concentration must be grossly inadequate in inducing ectopic bone. Observations by others support this hypothesis, when they found that application of BMP-2 at a delayed interval of 7 days after the time of surgery resulted in a significantly increased osteogenic induction [28] due to the increased number of BMP-2 responsive cells. However, in a separate study, fast release of BMP was associated with increased new bone induction over a short observation period, while a slow release was not [27]. Consequently, it appears that it is the release kinetics of BMP-2 with its net balance of effective concentration and degradation, which usually makes the difference. The release kinetic must be optimized for our chamber model, where a peak release is required at the time of rapid angiogenesis and FVT generation. Therefore, specifically for this A–V loop model, we may need a higher dosage of BMP-2 or later application during the course of the experiment. In the future, we propose a 2 week delay for BMP-2 application, where the burst release can be synchronized with presumptive maximum vascular tissue growth. Additionally, without proper mechanical stimulation, it is unlikely to find significant amounts of mature bone histologically or the induced bone might have even resorbed [36].

In comparison to growth factors, co-culture systems are attractive in addressing two components of a tissue such as the osteogenic compartment and blood vessels in bone tissue. Optimally, different cell components are capable of inducing each other to a fully differentiated state. However, regarding applications in regenerative medicine, autologous cells are the gold standard at the moment. Isolation and expansion of autologous cells under GMP conditions, which are mandatory for clinical application of bioartificial tissues, are technically demanding and rather expensive. Additionally, the bi-directional interaction of cells under co-culture conditions needs to be fully characterized. Large volume applications of bioartificial tissues are also hampered by significant initial cell loss if vascularization aspects are not considered. Growth factors such as BMPs might be utilized to enhance tissue formation and increase efficacy of cell based strategies [6]. Under certain conditions and in selected indications, they might even replace transplantation of cells if adequate release kinetics and material properties are provided.

Though the histological cut sections showed no bone formation, semi-quantitative real time PCR results showed a different picture of gene expression. Groups A (500 ng BMP-2) and C (osteoblasts) had significantly higher expression of bone-related genes especially, osteocalcin and IBSP. Group A also showed significantly increased expression of alkaline phosphatase. Expression of these bone-related genes is important at different stages of bone maturation. As histological bone formation is a very complex phenomenon, which requires coordinated interplay of different types of cells and growth factors, we assume that the osteo-inductive stimulus was sufficient to induce expression of bone-related genes but induction of bone formation eventually failed due to insufficient long-term concentration of BMPs and lack of effector cells. The expression of growth factors such as BMP-2, FGF-2, and VEGF were not significantly different at 8 weeks. Cell surface proteoglycans function in cell adhesion to cell or matrix. A higher expression of biglycan was found in group B (2.5 μg BMP-2), while there was no difference of Syndecan expression. Syndecan is ubiquitously expressed in all cells except for some bone-specific subtypes, while biglycan is highly expressed in bone morphogenesis [37]. Cell mitosis can occur at pico molar range of BMP-2, while cell differentiation needs nano molar range [9]. When BMP-2 is sequestered in extracellular matrix, local concentration might be higher to produce sporadic induction. This might explain the positive bone-related gene expression while absence of any clearly demarcated histological bone.

Although a well-vascularized scaffold is essential for the survival of osteoblasts, we have surprisingly found that the presence of cells is also crucial for development of extensive axial vascularization in a reciprocal manner. Therefore, the chamber model could be made porous in future by further modification to have access to the surrounding area, making both simultaneous extrinsic and axial vascularization possible at a very early stage.

The approach may not only induce survival and faster differentiation of osteoblasts but also stimulate in-growth of new blood vessels. Moreover, application of angiogenetic growth factors such as VEGF might have a similarly stimulating effect. As discussed earlier, BMP-2 and osteoblasts might be applied in pre-vascularized scaffold after 2 weeks delay for their most efficient action, which is currently under investigation by our group. Though such an approach makes the model complex, it may ensure the survival of cells and their differentiation from the beginning.

At present, each of the individual components of PLDLLA–TCP–PCL and Extracel-HP is approved by the FDA. Even so, as a whole group, the exact applicability of the current approach needs to be demonstrated. It might utilize a patient's body as a bioreactor to make a tissue engineered graft behave as an autograft to address the limitation of autograft availability and the associated morbidity in their procurement [11]. However, a number of issues must be addressed before this kind of therapeutic strategy can be applied.

In the future, BMP-2 loaded hydrogel might be highly active on nearby MSCs if BMP-2 is applied after complete growth of fibro-vascular tissue. Considering the well-established biomaterials and the huge demand of vascularized autografts in patients, a well-vascularized engineered bone might satisfy the unmet demand. As a vein graft can be utilized for induction of vascularization, this surgical approach might eventually allow generation of axially vascularized tissues with minimal donor site morbidity independently of anatomic vascular axis.

5 Conclusion

In this study, we demonstrated that BMP-2 may be contained within and slowly released from a Hyaluronan-based hydrogel for more than 5 weeks. The hydrogel along with PLDLLA–TCP–PCL scaffold could be axially vascularized by an A–V loop. The hyaluronan hydrogel was gradually degraded that guided sustained FVT growth and the released BMP-2 induced bone-related gene expression, although the formation of bone could not be observed histologically. Based on the results of this experiment, it can be concluded that the PLDLLA–TCP–PCL-hyaluronan scaffold containing BMP-2 and supplied with an A–V loop can possibly be explored as a well-vascularized bone graft after further optimization.

Acknowledgments This study was supported by research grants from the Deutsche Forschungsgemeinschaft (DFG) (KN 578/2-1) and the Xue Hong and Hans Georg Geis Foundation. The authors thank Dr. Andreas Hess, Institute of Experimental and Clinical Pharmacology and Toxicology for helping in micro-CT scanning and Prof. Peter Greil and Mr. Peter Reinhard for production of the Teflon chambers.

References

1. Pneumaticos SG, Triantafyllopoulos GK, Basdra EK, Papavassiliou AG. Segmental bone defects: from cellular and molecular pathways to the development of novel biological treatments. J Cell Mol Med. 2010. doi:10.1111/j.1582-4934.2010.01062.x.
2. Scheufler O, Schaefer DJ, Jaquiery C, Braccini A, Wendt DJ, Gasser JA, et al. Spatial and temporal patterns of bone formation in ectopically pre-fabricated, autologous cell-based engineered bone flaps in rabbits. J Cell Mol Med. 2008;12(4):1238–49. doi:10.1111/j.1582-4934.2008.00137.x.
3. Arkudas A, Tjiawi J, Bleiziffer O, Grabinger L, Polykandriotis E, Beier JP, et al. Fibrin gel-immobilized VEGF and bFGF efficiently stimulate angiogenesis in the AV loop model. Mol Med. 2007;13(9–10):480–7.
4. Reddi A. Bone morphogenetic proteins: from basic science to clinical applications. J Bone Joint Surg J. 2001;83(Suppl 1, Part 1):S1.
5. Arkudas A, Beier J, Heidner K, Tjiawi J, Polykandriotis E, Srour S, et al. Axial prevascularization of porous matrices using an arteriovenous loop promotes survival and differentiation of transplanted autologous osteoblasts. Tissue Eng. 2007;13(7):1549–60.
6. Kneser U, Schaefer DJ, Polykandriotis E, Horch RE. Tissue engineering of bone: the reconstructive surgeon's point of view. J Cell Mol Med. 2006;10(1):7–19.
7. Beier J, Horch R, Hess A, Arkudas A, Heinrich J, Loew J, et al. Axial vascularization of a large volume calcium phosphate ceramic bone substitute in the sheep AV loop model. J Tissue Eng Regen Med. 2010;4(3):216–23.
8. Ai-Aql ZS, Alagl AS, Graves DT, Gerstenfeld LC, Einhorn TA. Molecular mechanisms controlling bone formation during fracture healing and distraction osteogenesis. J Dent Res. 2008;87(2):107–18.
9. Reddi A. Role of morphogenetic proteins in skeletal tissue engineering and regeneration. Nat Biotechnol. 1998;16(3):247–52.
10. Eyckmans J, Roberts SJ, Schrooten J, Luyten FP. A clinically relevant model of osteoinduction: a process requiring calcium phosphate and BMP/Wnt signaling. J Cell Mol Med. 2009. doi:10.1111/j.1582-4934.2009.00807.x.
11. Terheyden H, Menzel C, Wang H, Springer IN, Rueger DR, Acil Y. Prefabrication of vascularized bone grafts using recombinant human osteogenic protein-1–part 3: dosage of rhOP-1, the use of external and internal scaffolds. Int J Oral Maxillofac Surg. 2004;33(2):164–72.
12. Patel VV, Zhao L, Wong P, Pradhan BB, Bae HW, Kanim L, et al. An in vitro and in vivo analysis of fibrin glue use to control bone morphogenetic protein diffusion and bone morphogenetic protein–stimulated bone growth. Spine J. 2006;6(4):397–403.
13. Seeherman H, Wozney J, Li R. Bone morphogenetic protein delivery systems. Spine (Phila Pa 1976). 2002;27(16 Suppl 1):S16–23.
14. Yamamoto M, Takahashi Y, Tabata Y. Controlled release by biodegradable hydrogels enhances the ectopic bone formation of bone morphogenetic protein. Biomaterials. 2003;24(24):4375–83.
15. Anitua E, Sánchez M, Orive G, Andia I. Delivering growth factors for therapeutics. Trends Pharmacol Sci. 2008;29(1):37–41.
16. Meyer R Jr, Gruber H, Howard B, Tabor O Jr, Murakami T, Kwiatkowski T, et al. Safety of recombinant human bone morphogenetic protein-2 after spinal laminectomy in the dog. Spine. 1999;24(8):747.

17. Bishop G, Einhorn T. Current and future clinical applications of bone morphogenetic proteins in orthopaedic trauma surgery. Int Orthop. 2007;31(6):721–7.
18. Pike DB, Cai S, Pomraning KR, Firpo MA, Fisher RJ, Shu XZ, et al. Heparin-regulated release of growth factors in vitro and angiogenic response in vivo to implanted hyaluronan hydrogels containing VEGF and bFGF. Biomaterials. 2006;27(30):5242–51. doi: 10.1016/j.biomaterials.2006.05.018.
19. Zhao B, Katagiri T, Toyoda H, Takada T, Yanai T, Fukuda T, et al. Heparin potentiates the in vivo ectopic bone formation induced by bone morphogenetic protein-2. J Biol Chem. 2006; 281(32):23246.
20. Zein I, Hutmacher DW, Tan KC, Teoh SH. Fused deposition modeling of novel scaffold architectures for tissue engineering applications. Biomaterials. 2002;23(4):1169–85.
21. Lam C, Olkowski R, Swieszkowski W, Tan K, Gibson I, Hutmacher D. Mechanical and in vitro evaluations of composite PLDLLA/TCP scaffolds for bone engineering. Virtual Phys Prototyp. 2008;3(4):193–7.
22. Yang J, Wan Y, Tu C, Cai Q, Bei J, Wang S. Enhancing the cell affinity of macroporous poly(L-lactide) cell scaffold by a convenient surface modification method. Polym Int. 2003;52(12): 1892–9.
23. Kneser U, Stangenberg L, Ohnolz J, Buettner O, Stern-Straeter J, Mobest D, et al. Evaluation of processed bovine cancellous bone matrix seeded with syngenic osteoblasts in a critical size calvarial defect rat model. J Cell Mol Med. 2006;10(3):695–707.
24. Kneser U, Polykandriotis E, Ohnolz J, Heidner K, Grabinger L, Euler S, et al. Engineering of vascularized transplantable bone tissues: induction of axial vascularization in an osteoconductive matrix using an arteriovenous loop. Tissue Eng. 2006;12(7): 1721–31.
25. Bolland BJRF, Kanczler JM, Dunlop DG, Oreffo ROC. Development of in vivo μCT evaluation of neovascularisation in tissue engineered bone constructs. Bone. 2008;43(1):195–202.
26. Arkudas A, Pryymachuk G, Hoereth T, Beier J, Polykandriotis E, Bleiziffer O, et al. Dose-Finding Study of Fibrin Gel-Immobilized Vascular Endothelial Growth Factor 165 and Basic Fibroblast Growth Factor in the Arteriovenous Loop Rat Model. Tissue Eng A. 2009;15(9):2501–11.
27. Talwar R, Di Silvio L, Hughes FJ, King GN. Effects of carrier release kinetics on bone morphogenetic protein-2-induced periodontal regeneration in vivo. J Clin Periodontol. 2001;28(4): 340–7.
28. Seeherman H, Li R, Bouxsein M, Kim H, Li X, Smith-Adaline E, et al. rhBMP-2/calcium phosphate matrix accelerates osteotomy-site healing in a nonhuman primate model at multiple treatment times and concentrations. J Bone Joint Surg. 2006;88(1):144.
29. Rothstein S, Federspiel W, Little S. A unified mathematical model for the prediction of controlled release from surface and bulk eroding polymer matrices. Biomaterials. 2009;30(8):1657–64.
30. Adams JR, Sander G, Byers S. Expression of hyaluronan synthases and hyaluronidases in the MG63 osteoblast cell line. Matrix Biol. 2006;25(1):40–6. doi:10.1016/j.matbio.2005.08.007.
31. Kakudo N, Kusumoto K, Wang YB, Iguchi Y, Ogawa Y. Immunolocalization of vascular endothelial growth factor on intramuscular ectopic osteoinduction by bone morphogenetic protein-2. Life Sci. 2006;79(19):1847–55. doi:10.1016/j.lfs.2006.06.033.
32. Toole BP, Hascall VC. Hyaluronan and tumor growth. Am J Pathol. 2002;161(3):745–7.
33. Mazumdar J, Dondeti V, Simon M. Hypoxia-inducible factors in stem cells and cancer. J Cell Mol Med. 2009;13(11–12):4319–28.
34. Jeon O, Song S, Kang S, Putnam A, Kim B. Enhancement of ectopic bone formation by bone morphogenetic protein-2 released from a heparin-conjugated poly(l-lactic-co-glycolic acid) scaffold. Biomaterials. 2007;28(17):2763–71.
35. Inoda H, Yamamoto G, Hattori T. rh-BMP2-induced ectopic bone for grafting critical size defects: a preliminary histological evaluation in rat calvariae. Int J Oral Maxillofac Surg. 2007;36(1): 39–44.
36. Murakami T, Saito A, Hino S, Kondo S, Kanemoto S, Chihara K, et al. Signalling mediated by the endoplasmic reticulum stress transducer OASIS is involved in bone formation. Nat Cell Biol. 2009;11(10):1205–11. doi:10.1038/ncb1963.
37. Lamoureux F, Baud'huin M, Duplomb L, Heymann D, Redini F. Proteoglycans: key partners in bone cell biology. BioEssays. 2007;29(8).